

Desulfurization of gas oil using a solar photocatalytic microreactor

Mohammad Fadhil Abid

Chemical Engineering Department, University of Technology, Baghdad, Iraq

Abstract

The present work is devoted to investigate the performance of a homemade Y-shape catalytic microreactor for degradation of dibenzothiophene (DBT), as a model of sulphur compounds including in gas oil, utilizing solar incident energy. The microchannel was coated with TiO₂ nanoparticles which were used as a photocatalyst. Performance of the microreactor was investigated using different conditions (e.g., DBT concentration, LHSV, operating temperature, and (H₂O₂/DBT) ratio). Our experiments show that, in the absence of UV light, no reaction takes place. The results revealed that outlet concentration of DBT decreases as the mean residence time in the microreactor increases. Also, it was noted that operating temperature showed a positive impact on the degradation rate of DBT while LHSV showed a different image. The results reported an optimum (H₂O₂/DBT) ratio which gave maximum conversion of DBT which vary with initial concentration. Kinetic study was carried out which confirmed that desulfurization of DBT followed a pseudo-first order reaction at 30 and 50°C, respectively. However deviation from linearity was observed at 60°C. Comparison between microreactor's performance and performance of batch reactors from published literature were illustrated. The Comparison confirmed the unique characteristics of the microreactor.

Key Words: Microreactor, Solar energy, photocatalysis, desulfurization, dibenzothiophene

Introduction

Crude oil is the largest and most widely used source of energy in the world. Major portions of the crude oils are used as transportation fuels such as gasoline, diesel and jet fuel. However, such crudes contain sulfur, typically in the form of organic sulfur compounds. The sulfur content and the API gravity are two properties which have a great influence on the value of the crude oil. The sulfur content is expressed as a percentage of sulfur by weight and varies from less than 0.1% to greater

than 5% depending on the type and source of crude oils [1]. Combustion of gasoil and diesel fuel has been identified as one of the major emission sources of polyaromatic hydrocarbons (PAH) in urban areas. As environmental consciousness rises, all countries worldwide introduce more stringent legislation to limit the PAH content of diesel fuels. In the foreseeable future, a sulfur content as low as 10 ppm and a PAH content not greater than 2% may be proposed in most countries worldwide.

Furthermore, the sulfur compounds are taken into account as the components of PAH. Dibenzothiophene (DBT) and its derivatives are the major sulfur species in diesel and gas oil [2]. Currently, hydrosulfurization (HDS) is used to remove sulfur from hydrocarbons in petroleum refineries which require either increasing reactor residence time, or carrying out reactions in severe conditions [3]. The catalysts used in HDS are not active in removing refractory sulfur compounds, such as dibenzothiophenes (DBTs) and its derivatives, and these compounds require higher hydrogen consumption in the HDS process [1].

In the past few years, microreactor technology is presented as a novel and breakthrough technology on which the new concept of production and research will be built upon. The chemical industry, biotechnology, pharmaceutical industry and medicine, life science, clinical and environmental diagnostic are just some of the small fields where this new concept in production, analysis and research could find its place of application [4]. By decreasing the equipment size by several magnitude levels, substantial economic benefits, improvement of intrinsic safety, and a reduction of environmental impact can be achieved [5]. The large surface area, per volume, gives high thermal conductivity to a micro-channel allowing quick and accurate temperature control of the chemicals inside [6]. Recent reports have demonstrated that a vast range of organic reactions - including the aldol reaction [7], the synthesis of esters [8], the Hantzsch synthesis [9], and fluorinations [10], chlorination [11] and brominating [12] - can be performed within microreactors.

Microreactors can be manufactured from metal, glass, and a range of polymeric materials [13]. A number of

techniques may be used to create the required network of microchannel, including photolithographic, moulding, embossing and milling processes [14]. In the field of bio-catalysis, Drott et al. [15] have investigated the use of porous silicon as a carrier matrix in microstructured enzyme reactors, increasing the surface area onto which enzymes could be coupled, using the microreactor fabricated at 50 mA/cm² current density, they found that the enzyme activity was increased 100-fold compared with the reference reactor. Chambers et al. [16] have reported the development of a microreactor in which elemental fluorine has been used to allow both the selective fluorination and per fluorination of organic compounds in a simple controllable manner. The synthesis of fluorine-containing organic compounds has many inherent safety issues such as safe handling and temperature control. (Chambers et al. [16] outlined the potential benefits of the microreactor used as being (i) a small inventory of fluorine in the reaction zone, (ii) an opportunity for good mixing and temperature control and (iii) simple reaction scale-up. Kelly et al. [17] developed a system of a microreactor in combination with a micro fuel cell as an alternative to conventional portable sources of electricity such as batteries due its ability to provide an uninterrupted supply of electricity as long as a supply of methanol and water can be provided. They proved that the energy storage density per unit volume/weight of this system was higher than that of batteries, which translates into less frequent recharging through the refilling of methanol fuel. The large surface area, per volume, gives high thermal conductivity to a micro-channel allowing quick and accurate temperature control of the chemicals inside [6]. There are a lot of chemical

systems using micro-channels. Many of them are made of transparent material, such as glass, plastics, or silicone rubber, so the researchers can visually observe the reactions [18, 19]. The desulfurization reaction is most often considered as a pseudo 1st order rate reaction [20]. The pseudo 1st order approximation is associated with the overall degradation reaction of dibenzothiophene which may be assumed to consist of the following steps [20],
activation of substrate:



activation of oxidant:



substrate conversion with activated oxidant:



where T and hv represent the organic substrate and UV photon energy, respectively.

In the above degradation pathway, all the radicals formed by the collision of one photon and one molecule of H₂O₂ are included in the term H₂O₂*. H₂O₂ itself does not oxidize DBT in the absence of UV light; but it helps the excited DBT molecules to be oxidized [21].

The aim of the present work was to investigate the desulfurization of gas oil utilizing a solar photocatalysis microreaction process. Influence of the operating variables such as initial sulfur content, inlet mixture flow rate, and H₂O₂ loadings on reactor performance was investigated. In addition, the kinetic parameters of the desulfurization process were estimated.

Materials and Methods

Materials

The chemicals which have been used in this work are: Titanium dioxide ((TiO₂, 80% anatasa) of Size (5-30nm) (specific surface area 60±15 m²/g (BET), was obtained from Zhengzhou Xinyue Chemical Co., China.). Dibenzothiophene (purity 97%, from Riedel-de Haën AG, Germany) was used as a model for the sulfur containing compounds in the fuel. N-hexane (purity 85%) was used as a carrying medium inside the microreactor for dibenzothiophene. N-Hexane was obtained from Merck Millipore, Malaysia. Deionized water and acetonitrile from LabScan- Poland were used as a mobile phase in the HPLC. The mobile phase prepared from (70% acetonitrile, 30% water). The hydrogen peroxide solution which is used as the oxidizing agent (purity35%) was obtained from Merck-Gruppe, Germany. All chemicals are HPLC grade and were used as received without further purification.

Microreactor design and fabrication

For the design of a micro reactor, it has to be considered that both heat and mass transport time-scales are strongly correlated with the characteristic dimensions of the microreactor according to diffusion theory [22, 23]:

$$\text{Heat transport: } t \sim l^2/a \sim L/u \dots\dots(4)$$

$$\text{Mass transport: } t \sim l^2/D \sim L/u \dots\dots(5)$$

$$l^2/a \cdot t = l^2 \cdot u / a \cdot L \sim 1 \dots\dots\dots(6)$$

$$l^2/D \cdot t = l^2 \cdot u / D \cdot L \sim 1 \dots\dots\dots(7)$$

where

L: travelling length, t: time-scale, l: diffusion length, a: thermal diffusivity of fluid, D: mass diffusivity, u: flow speed

The first step is diffusing to a reactive surface followed by the reaction. The diffusion time is one of the principal factors on how fast conversion can be accomplished. Various approaches have been applied to simulate the flow in different types of microreactor and to estimate the optimum dimensions [24-26]. To estimate the main dimensions of the microreactor (i.e., width and length of the microchannel and the angle between the lateral channel and the central line of the main channel), the governing equations for the fluids (i.e., continuity, momentum, and concentrations) are solved using MATLAB Version 7. The physical properties, operating parameters of the system (D , μ , ρ , a , and u), and equations (6) and (7) are inserted together with the required boundary conditions to obtain the optimum dimensions.

Y-shape microreactor was drawn using 2D AUTOCAD and fabricated using SURFCAM software on CNC milling machine type C-tek. The schematic diagram shown in Fig. 1 displays the dimensions of the reactor pattern. This reactor design has the advantage of independent control and monitoring of the reactant and product streams. It also provides in situ mixing of reactants, thus avoiding some of the hazards associated with a premixed feed. The mixing efficiency of the Y-junction depends on flow rates, nature of the reactant molecules and channel aspect ratio (width/height).

Fig. 2 shows the microreactor which was fabricated in the Training and Workshops Centre-University of Technology. The upper and lower parts of the reactor were made of transparent elastic polydimethylsiloxane (PDMS) and aluminium alloy, respectively. A transparent flexible gasket was inserted between the two parts before bolted with each other.

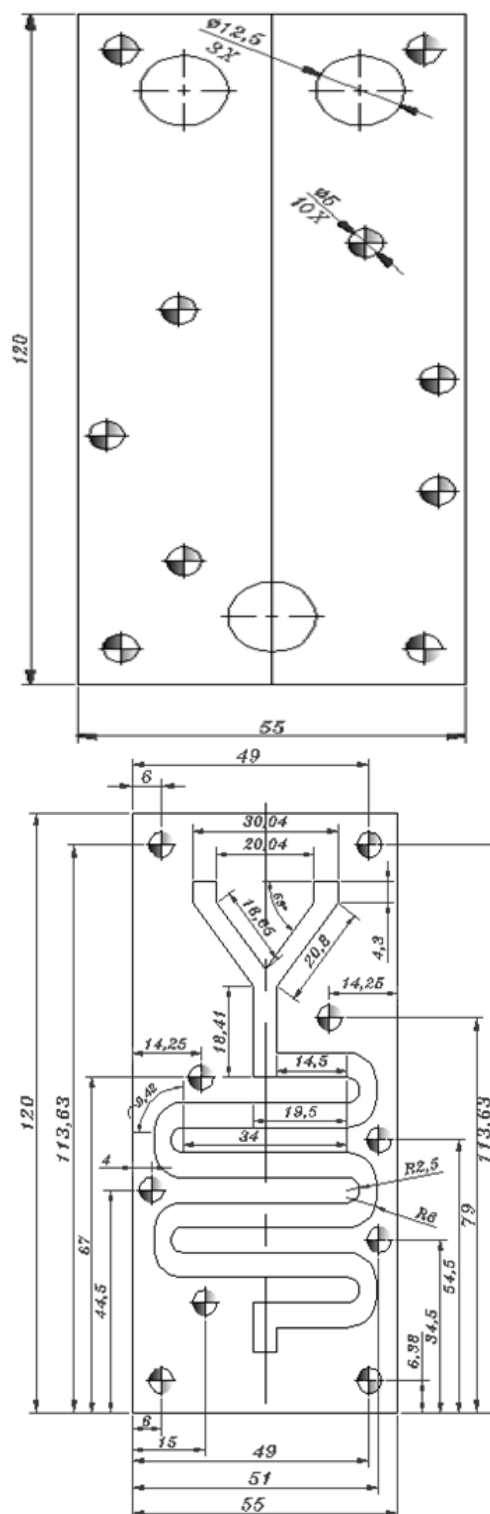


Fig. 1, Dimensional schematic of the microreactor pattern (all dimensions are in mm)

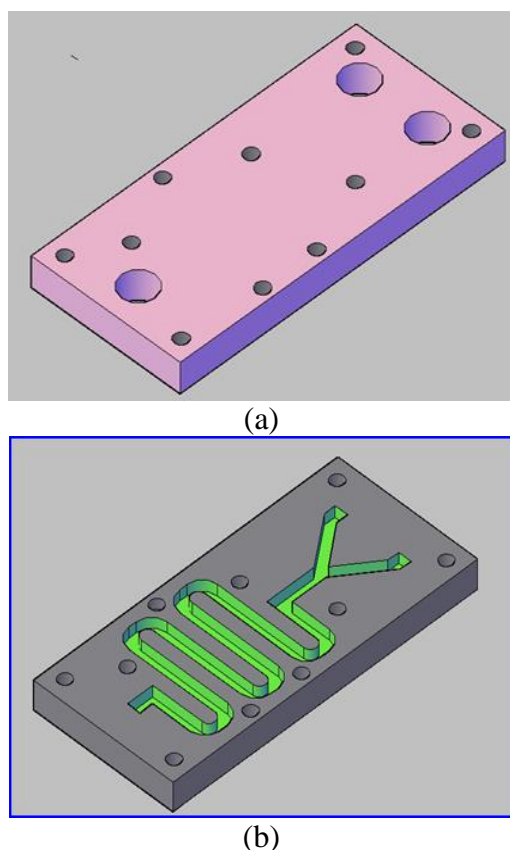


Fig. 2, Disassembly of the microreactor (a) upper part, (b) lower part

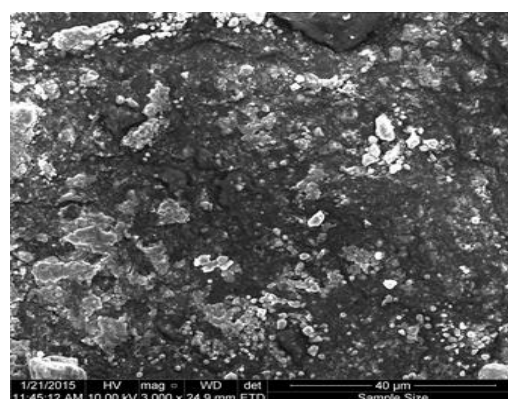
Catalyst

Deposition of nano-TiO₂ particles on microchannel of the aluminium plate, in the present research was performed as follows:

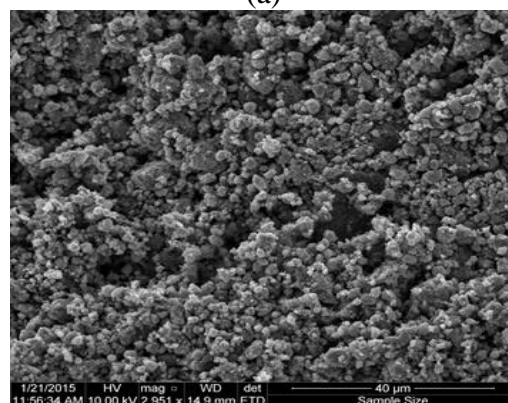
1. In a beaker, 1.5 mL of a dilute nitric acid solution (pH = 3.5) and 4.5 mL of 50% ethanol and 0.5 g nano-TiO₂ powder were added while stirring by a magnetic stirrer at 300 rpm. Before deposition, the surface was washed in a basic solution of NaOH in order to increase the number of OH groups.
2. After 15 minutes of stirring, a given volume suspension was carefully injected in the microchannel using a 5-ml syringe. The suspension filled the microchannel and allowed to dry at 80°C for six hours.
3. The coated sample was then annealed for 30 minutes at 350°C. During the heating, OH groups

from the catalyst surface and the support can react and lose a molecule of water, creating an oxygen bridge, thus increasing the adherence of the catalyst to the support.

4. This deposition process could be carried several times in succession so as to increase the total thickness. Microchannel was scanned using SEM (model Inspect S50, S/N 9922650, FEI Company, USA) to investigate the effect of successive coatings on microchannel as shown in Figure 4. The first coat does not cover the entire surface but additional coats lead to a complete coverage. Scanning procedure was carried out at the Applied Sciences Department-University of Technology.



(a)



(b)

Fig. 3, Effect of successive coating of microchannel with nanoTiO₂, after first coating (a) and after third coating (b)

Experimental setup

Figure 4 presents a schematic diagram and a photographic view of the experimental setup is shown in Fig.5 (a, and b).

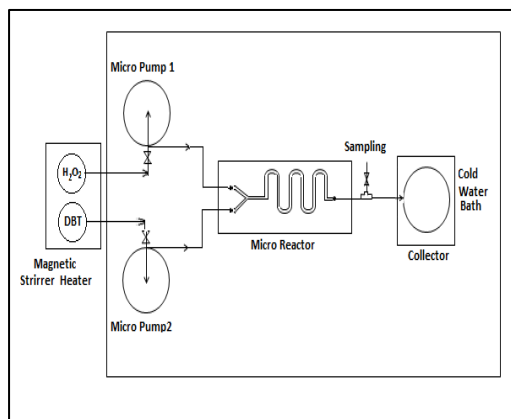
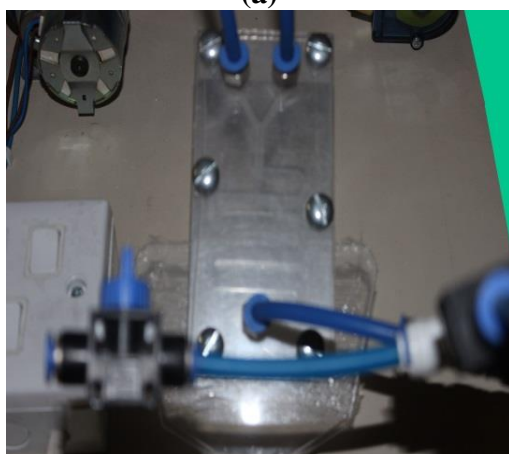


Fig. 4, Schematic of the experimental setup



(a)



(b)

Fig. 5, Photographic view of the setup (a) and the microreactor (b)

A solution of certain concentration of dibenzothiophene in hexane was prepared and contained in a 250 ml graduated glass serum container connected to a micropump via a regulating valve. Another 250 ml graduated glass serum container filled with a 30% hydrogen peroxide solution was connected to a second micropump. The two containers were installed on a magnetic stirrer supplied with an electric heater to keep the homogeneity of the mixture in a steady form and heating the feeds to a desired initial temperature. Valves were calibrated with the level in each container so different flow rates could be delivered to the microreactor separately in each run. Each micropump manufactured by Williamson Company Limited, model number 200.015.230.016 was used to deliver the feed (reactants) to the microreactor. Effluent of the microreactor was collected in a graduated 250 ml container surrounded by a cold water bath. Just at the exit of the microreactor the experimental setup was supplied with a valve for instantaneous sampling. The sample was centrifuged to separate the water contained in H_2O_2 and the upper solution was injected to the HPLC (HPLC–UV; Agilent Technologies 1100; a C-18, (25 cm x 4.6 mm i.d.) stainless steel column (packed with Zorbax 8- μ m, ODS- bound, spherical, silica particles) and was used with a mobile phase consisting of 70% Acetonitrile and 30% Water flowing at a rate of 1ml/min) to find out the unreacted dibenzothiophene concentration in hexane. All containers and tubing outside the microreactor were shielded from UV-exposure. Flowrates of 0.75, 1, 1.5, 2 l/min were used which correlate to 8.1, 6.1, 4, 3min residence times. The fractional degradation (x) of DBT was calculated by eqn. 8:

$$\text{Fractional degradation (x)} = (C_0 - C(t))/C_0 \dots (8)$$

Procedure

To analyze the dibenzothiophene concentration, an HPLC was used in this study. A series of dibenzothiophene/hexane solutions at concentrations of 20, 50, 100, 200, 300, and 500 ppm are used to generate calibration curves. Before analysis, each solution was diluted by a factor of 1:10; this dilution is done because of the *limitations* in the HPLC. Similar analytical methods used by others use a mobile phase of Acetonitrile and water, Acetonitrile, Tetrahydrofuran, and

water, or Methyl Hydroxide and water [27]. In the present work, the mobile phase used was 70:30 Acetonitrile to water ratio with the C-18 column on hand. Figure 6 shows a chromatograph of dibenzothiophene of 400 ppm concentration in hexane with a retention time of 9.93 min. The calibration curve of the dibenzothiophene/hexane solution for area vs. concentration (ppm) is shown in Fig. 7 This curve correlate a given peak area with a known concentration.

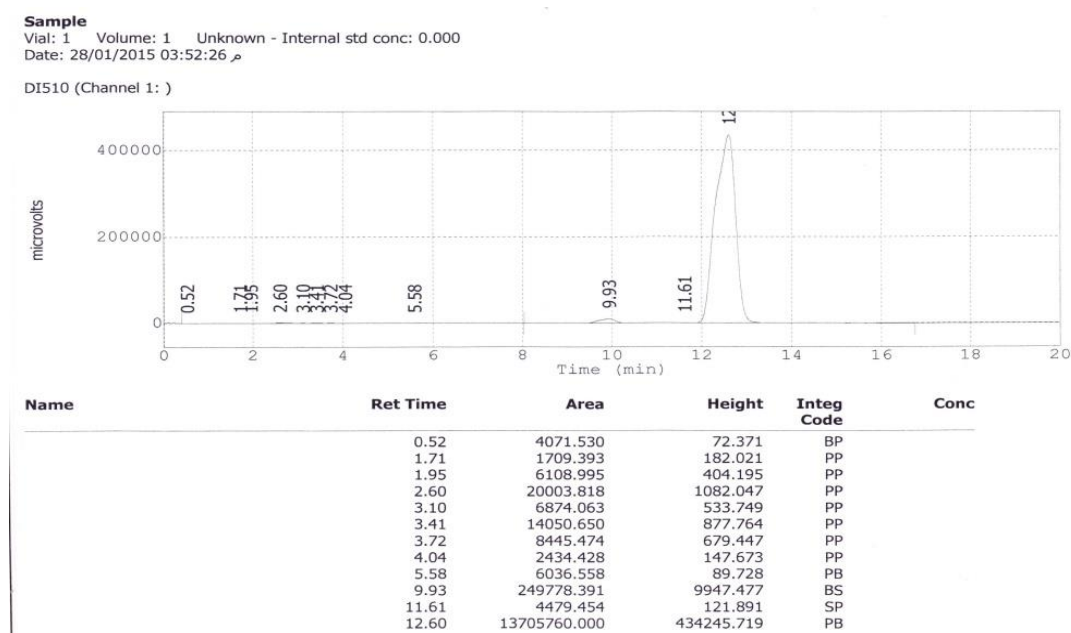


Fig. 6, chromatograph of dibenzothiophene

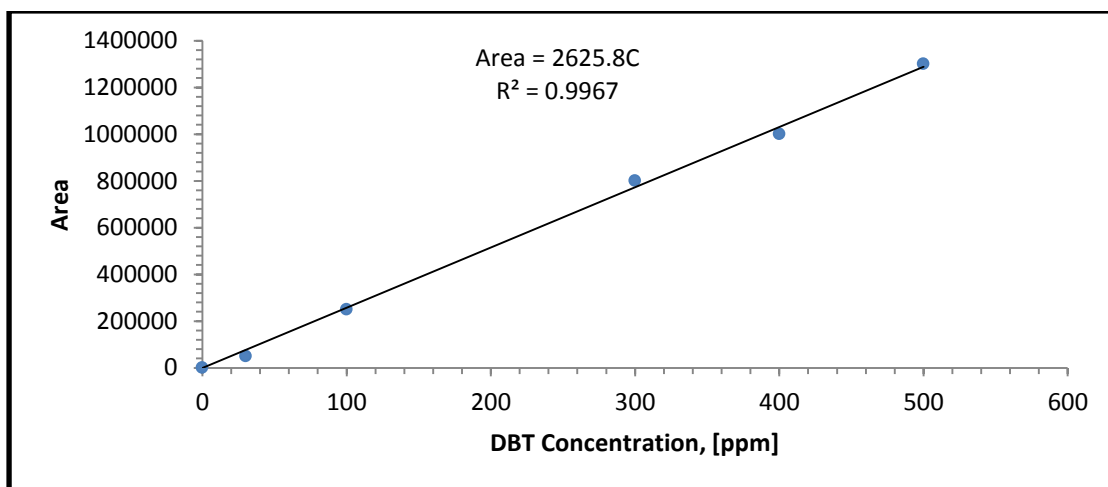


Fig. 7, Calibration curve of dibenzothiophene

Results and Discussion

Influence of Solar Incident Energy on Desulfurization Process

To investigate the influence of the incident solar energy on reaction mechanism of DBT, an amount of 500 ppm of DBT in hexane solution that was used as the feed to the microreactor was mixed with an equal amount of 30% hydrogen peroxide solution and placed in a serum bottle. The bottle is kept at a temperature of 5°C for three hours in a cold water bath. The concentration of DBT in hexane was followed with time as shown in Fig.8. Fig. 8 indicates no apparent change in the concentration of DBT and this revealed that the desulfurization reaction was taking place only inside the microreactor where the materials were illuminated by the UV light. This finding supports and proves that the suggested reaction mechanism that hydrogen peroxide itself does not directly oxidize dibenzothiophene for sulfur removal but it helps the photo excited dibenzothiophene to be oxidized.

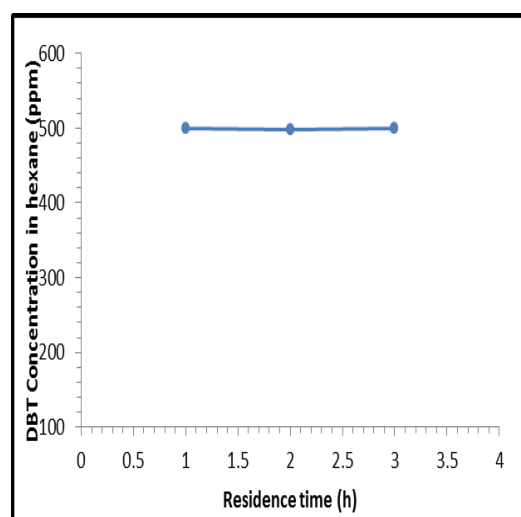


Fig. 8, Concentration of DBT in hexane vs. time for a sample of stoichiometric ratio of H₂O₂:DBT in a container at 10 °C and C₀=500 ppm DBT

Influence of Concentration of DBT

Figure 9 represents the experimental results conducted for DBT desulfurization at different space times. Again, it is observed that the outlet concentration decreases as the mean space time inside the microreactor increases. This confirms the fact that if the DBT stays longer in the reactor, its conversion increases as the space time increases. The effect of initial concentration of DBT solution on DBT degradation efficiency has been investigated by varying the DBTs concentration from (100 to 500 ppm). Fig. 9 also plots the variation of DBTs degradation against residence time in the presence of TiO₂ nanoparticles under solar light. As can be seen from Fig. 9 that after 8.1 min of irradiation time the degradation was 65%, 58%, and 40% at DBT concentrations of (100, 300, and 500 ppm), respectively. DBT degradation rate was observed to decrease as initial concentration increased.

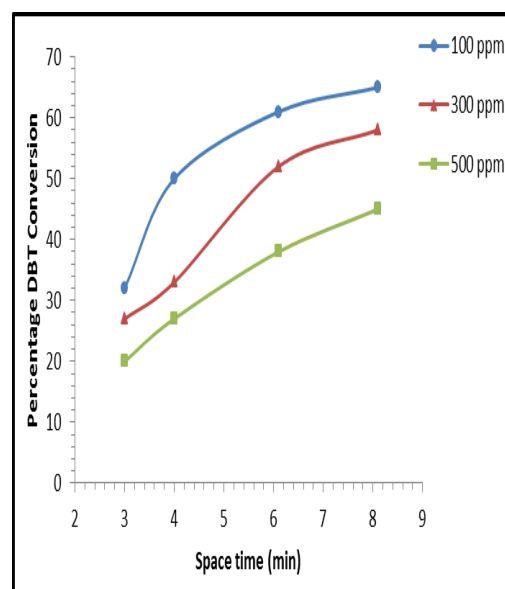


Fig. 9, Variation of DBT conversion against residence time at different concentrations of DBT, initial temperature= 50°C, (H₂O₂/DBT)=1

Influence of Initial Temperature and LHSV

Fig. (10), illustrates the effects of reaction temperature and space velocity of the influent stream on the reduction of DBT. An increase in the reaction temperature was observed to result in increased removal of DBT. The effect of temperature was to increase the specific rate constant which pronounced the conversion. As can be seen from Fig. 10, the removal of DBT was shown to decrease markedly as LHSV of the influent stream increased this may be due to the retention time during the oxidation process which was reduced.

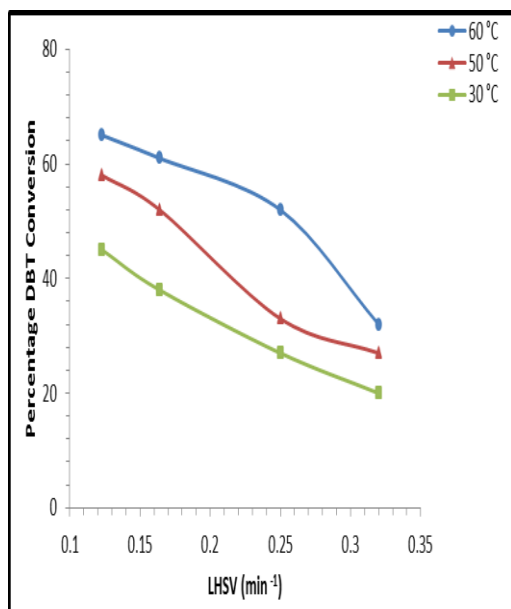


Fig. 10, Effect of initial temperature and LHSV on DBT conversion (DBT concentration =100 ppm, (H₂O₂/DBT) =1)

Influence of Molar Ratio of H₂O₂/DBT

Fig. (11), shows the variation of normalized DBT concentration against H₂O₂/DBT ratio in solution, keeping all other parameters unchanged. Different (H₂O₂ /DBT) ratio (1 to 6) was used to study the effect of H₂O₂ concentration on the desulfurization rate. As can be seen, the removal rate increased with increasing initial

concentration of H₂O₂ at fixed concentration of DBT. The desulfurization rate was slow at low H₂O₂ concentration, as the formation of hydroxyl radicals was insufficient; this may be explained by the ability of H₂O₂ to trap the electrons, preventing the electron-hole recombination and hence increasing the chance of formation of OH* radicals on the surface of the catalyst [28]. However, at a DBT concentration of 100 ppm, as the H₂O₂/DBT ratio increased beyond a certain limit, (4), the increased decomposition rate became noticeably less. This trend was also observed for DBT concentration of 300 and 500 ppm but at a H₂O₂/DBT ratio of 5 and 6, respectively. This was because at higher H₂O₂ concentration, more OH* radicals were produced leading to a faster oxidation rate. However, these excess free radicals were more prone to react with the excess H₂O₂ rather than with the DBT [29]. One form of this effect can be seen through short-circuiting the semiconductor microelectrode [30], according to eqn. (9) and (10):

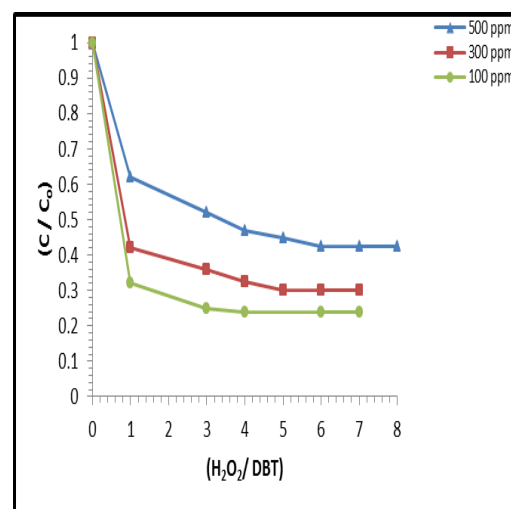
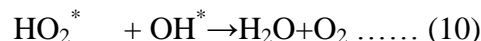
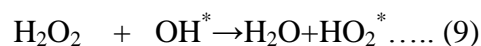


Fig. 11, Variation of normalized concentration against (H₂O₂/DBT) at different DBT concentrations

Therefore, it is imperative to determine the stoichiometric amount of hydrogen peroxide sufficient for complete mineralization. This analysis was not presented in the present work.

Kinetics study

Kinetics studies were carried out under optimal reaction conditions. The rate constant for the apparent consumption of DBT was obtained from the pseudo first-order eqn. 11:

$$r = -dC/dt = kC = k_1 C_0 (1-x) \dots\dots(11)$$

$$r = C_{A0} dx/dt = k_1 C_0 (1-x) \dots\dots (12)$$

Eqn. 12 can be integrated between t= 0 and t= t, yielding:

$$\ln (1-x) = -k_1 t \dots\dots\dots (13)$$

Where *x* is the fractional degradation of DBT, *t* is the residence time (min), *k₁* is the first-order rate constant (s⁻¹), *C_o* is the initial concentration of DBT, and *r* is the reaction rate (mg DBT/cm³ cat. s).

When (-ln (1-x)) was plotted against *t*, a straight line was fitted to the data of Fig. 12 at 30°C and 50°C with correlation coefficient (R²) of 0.99 and 0.98, respectively. This suggested that DBT photo degradation reaction followed pseudo first-order kinetics. The reaction rate constants were found to be 1.17x10⁻³ s⁻¹ and 1.76x10⁻³ s⁻¹ at 30°C and 50°C, respectively. However, it is worth to mention that as operating

temperature increased above 50°C, a deviation from linearity trend of reaction order is resulted as reported in Table 1. Table 2 lists data related to the results of present work and to the information extracted from published literature.

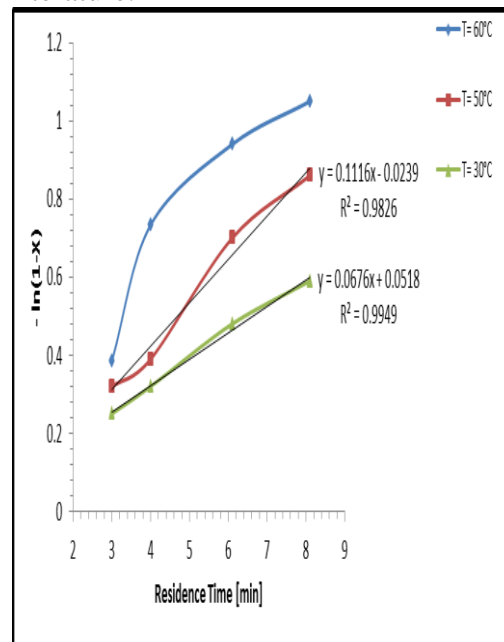


Fig.12, [-ln(1-x)] against residence time at different temperatures for kinetic study analysis, C_{DBT} =100 ppm and (H₂O₂/DBT) =4

Table (1), Results of kinetic study at C_{DBT} =100 ppm and (H₂O₂/DBT) =4

No.	Temperature	Reaction rate law (mg/g-cat.s)
1	30	1.17*10 ⁻³ C
2	50	1.76* 10 ⁻³ C
3	60	2.16*10 ⁻³ C ^{1.15}

Table 2: Data related to the results of present work and to the information extracted from published literature

Substrate	Desulfurization process	rate constant, s ⁻¹	Reactor type	Reference
DBT	Oxidative (30%H ₂ O ₂)+UV lamp	2.86x10 ⁻⁵ (at 50°C)	Batch reactor	Shiraishi et al. [31]
DBT	Oxidative (30%H ₂ O ₂)+UV lamp	1.61x10 ⁻³ (at 25°C)	(L. C. model SL-3) microreactor	Al-Raie [24]
DBT	Oxidative (30%H ₂ O ₂)+UV lamp	3.5x10 ⁻⁵ (at 50°C)	Batch reactor	Hirai et al. [21]
DBT	Solar photocatalysis	1.17x10 ⁻³ (at 30°C)	Y-shape microreactor	Present work

Comparison with Other Researchers' Works

Fig. 13 illustrates the comparison of the results obtained by other researchers for desulfurization of dibenzothiophene with the performance results obtained in the microreactor of the present work, and Table 3 summarizes the results obtained with different authors. Curve of Gemma [32] shows the profile of dibenzothiophene desulfurization by enzymatic effect of manganese peroxidase (MnP) on a 6 mg/l of DBT in a 100 ml batch reactor operated at 22°C. The degradation profile shows a conversion of 39% achieved after 8 hours of bio-treatment. Curve of Shiraishi et al. [31] shows the concentration profile for dibenzothiophene desulfurization with 30% hydrogen peroxide and solar UV light at $\lambda > 280$ nm in a batch reactor. A conversion of 82% is achieved after 8 hours of irradiation. The Curve of the present work shows a conversion of 65% achieved after 8.1 minutes of irradiation. It is evident from Table 3

that the microreactor was much more efficient for the desulfurization of dibenzothiophene as was anticipated due to understanding the advantages of microreactors.

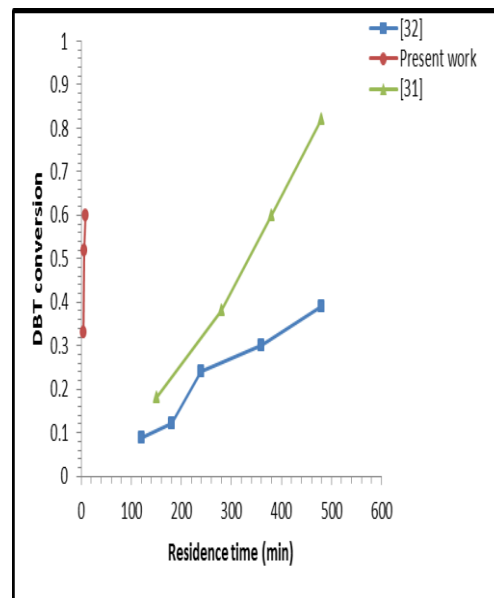


Fig. 13, Comparison between microreactor's performance and performance of batch reactors of Shiraishi et al. [31] and Gemma [32]

Table (3), Comparison between microreactor's performance and performance of batch reactors of Shiraishi et al. [31] and Gemma [32]

Substrate	Process	Type of reactor	Retention time	Conversion %	Reference
DBT	H ₂ O ₂ +UV lamp	Batch	480 min	82	[31]
DBT	Bioprocess	Batch	480 min	39	[32]
DBT	Solar photocatalysis	Y- shape microreacto	8.1 min	65	Present work

Conclusion

Recently, microreactor technology is presented as a novel and breakthrough technology on which the new concept of production and research will be built upon. In the present study desulfurization of dibenzothiophene in a solar photocatalysis microreactor was investigated. Results show that, in the absence of UV light, no reaction takes place. Experiments confirmed that the outlet concentration of DBT decreases

as the mean residence time in the microreactor increases. This is obvious because as dibenzothiophene remain longer in the reactor and thus their conversion increase with time. The reaction rate constant (k) was determined and found to be of the order of 10^{-3} (s⁻¹) for dibenzothiophene desulfurization. When this result is compared to reaction rate constants reported by other Investigators we find that this reaction proceeds much

slower in a batch reactor than in the microreactor. The degradation reaction of DBT exhibited a first order behaviour at 30 and 50°C, respectively. However the image was different at 60°C. This revealed the effect of temperature on the reaction order of desulfurization reaction. The experimental results obtained from the microreactor study were compared with the work reported by other researchers in this field. It was found that the microreactor is much more efficient than batch reactors for the desulfurization process of dibenzothiophene. This is an anticipated outcome based on the understanding of the advantages of microreactors in performing reaction processes in which mass transfer components play important role. In this study the microreactor was capable of achieving a 65% conversion of DBT in approximately 8.1 (min) which compares to approximately 340-500 (min) for a macroscopic batch reactor operation.

Acknowledgement

The author is thankful to the Department of Chemical Engineering-University of Technology for providing facilities and space where the present work was carried out. The author acknowledged the support of technical staff of the training and workshops centre- University of Technology.

Nomenclature

a thermal diffusivity of fluid (cm^2/s)
 C instantaneous concentration of DBT (ppm)
 C_0 initial concentration of DBT (ppm)
 D mass diffusivity (cm^2/s)
 DBT dibenzothiophene
 $h\nu$ UV photon energy (J)
 HDS hydrosulfurization

k_1 reaction rate constant (s^{-1})
 l diffusion length (cm)
 L travelling length (cm)
 L.C. liquid cell
 PAH polyaromatics
 r reaction rate of DBT (mg DBT reacted/ gm catalyst. s)
 SEM scanning electron microscope
 t time-scale (s)
 T organic substrate of equation (1)
 T^* organic substrate activated by UV photon
 u flow speed (cm/s)
 x fractional degradation of DBT

References

1. Fadhel Z. S., Desulfurization of Light Diesel Fuel Using Chloramine T and Polymer Supported Imidation Agent, MSc thesis, Chemical Engineering Department, University of Technology, Baghdad (2010).
2. Ting-Mu C., Chih-Ming W., Ikai W., Tseng-Chang T., Promoter effect of vanadia on Co/Mo/Al₂O₃ catalyst for deep hydrodesulfurization via the hydrogenation reaction pathway. *Journal of Catalysis* 272 (2010) 28–36.
3. Al-Malki A., Desulfurization of Gasoline and Diesel Fuels, Using Non-Hydrogen Consuming Techniques, M.Sc. Thesis, King Fahad University of Petroleum and Minerals, October, (2004)
4. Anita Š., Ana T., Bruno Z., Review: Application of microreactors in medicine and biomedicine, *Journal of Applied Biomedicine*. 10: 137–153, 2012.
5. Rebrov E.V., Duinkerke S.A., Croon M.H.J.M., Schouten J.C., Optimization of heat transfer characteristics, flow distribution, and reaction processing for a microstructured reactor/heat-exchanger for optimal performance

- in platinum catalyzed ammonia oxidation. *Chem Eng J.* 93: 201–216, 2003.
6. Kusakabe K., *J. of Chem. Eng. of Jpn.*, Vol. 35, No. 9, pp. 914-917, (2002)
 7. Wiles C., P. Watts, S. J. Haswell and E. Pombo-Villar, The aldol reaction of silyl enol ethers within a micro reactor, *Lab on a Chip*, 2001, 1, 100-101
 8. Wiles C., P. Watts, S. J. Haswell and E. Pombo-Villar, Solution phase synthesis of esters within a micro reactor, *Tetrahedron*, 2003, 59, 10173-10179.
 9. Garcia E. E., S. Y. F. Wong, B. H. Warrington, A Hantzsch Synthesis of 2-Aminothiazoles Performed in a Microreactor System, *Micro Total Analysis Systems 2001*, Proceedings of the μ TAS 2001 Symposium, held in Monterey, CA, USA 21–25 October, 2001, p 517-518, Editors: J. Michael Ramsey, Albert van den Berg.
 10. Hideki A., Aiichiro N. and Jun-ichi Y., Flow microreactor synthesis in organo-fluorine chemistry, *Beilstein J. Org. Chem.* (2013), 9, 2793–2802.
 11. Matsubara H., Y. Hino, M. Tokizane, and I. Ryu, Microflow Photo-Radical Chlorination of Cyclohexane, *Chemical Engineering Journal*, (2011), 167(2-3); 567-571,
 12. Löwe H., Bromination of Thiophene in Micro Reactors, *Letters in Organic Chemistry*, 11/2005; 2(8):767-779, Bentham Science Publishers.
 13. Wang Y., editor, and Holladay J. D., editor, *Microreactor Technology and Process Intensification*, ACS symposium; 914, (2003), ISBN 0-8412-3923-1
 14. Yuan-Chien T., Shung-Jim Y., Hsun-Tsing L., Hsiu-Ping J. and You-Zung H., Fabrication of a Flexible and Disposable Microreactor Using a Dry Film Photoresist, *Journal of the Chinese Chemical Society*, (2006), 53, 683-688
 15. Drott J., K. Lindstrom, L. Rosengrent, T. Laurell, J. Micromech. *Microeng.* 7 (1997) 14-23, UK.
 16. Chambers, R. D., and Spink, R. C. H., Microreactors for elemental fluorine, *Chem. Commun.* (1999) 883.
 17. Kelly S., G. Deluga, and W. Smyrl, Miniature fuel cells fabricated on silicon substrates, *AIChE.*, vol. 48, pp. 1071-1082, (2002)
 18. Fujinami M., M. Tokeshi, T. Odake, T. Kitamori, Sato K., T. Sawada, K. Matsumoto, M. Nakao, T. Ooi, and Y. Hatamura, Microfabricated Channels and Fluid Control Systems for Integrated Flow Injection Analysis, *Micro Total Analysis Systems 1998*, pp. 339-342 (1998)
 19. Takeshi O., Okabe Y., M. Nakao, and K. Iwata, Laminated Electrodes Chips for Pulse-Immunoassay, *Micro Total Analysis Systems 2002*, pp. 121-123 (2002).
 20. Arantegui J., Prado J., Chamarro E., and Esplugas S., Kinetics of the UV degradation of atrazine in aqueous solution in the presence of hydrogen peroxide, *J. Photochem. Photobiol. A: Chemistyr*, 88 (1995) 65-74.
 21. Hirai T., K. Ogawa, Y. Shiraishi, and I. Komasaawa, Effect of Photosensitizer and Hydrogen Peroxide on Desulfurization of Light Oil by Photochemical Reaction and Liquid-Liquid Extraction, *Ind. Eng. Chem. Res.*, (1997), 36, 530-533.
 22. Wegeng R.W., Call C.J. and Drost M.K., Proc. 1996 Spring National

- Meeting, AIChE, Feb. 25–29 New Orleans, Seiten 1–13.
23. Branbjerg J, Gravesen P., Krog J.P., and Nielsen C.R., Proc. IEEE MEMS '96, San Diego, USA (1996)
24. Ali H. Al-Raie, Desulfurization of Thiophene and Dibenzothiophene with Hydrogen Peroxide in a Photochemical Microreactor, MSc thesis, Oregon State University, 2005
25. Wang X., Hirano H, Xie G., and Ding X., VOF Modeling and Analysis of the Segmented Flow in Y-Shaped Microchannels for Microreactor Systems, *Advanced in High Energy Physics*, Vol. 2013, Article ID 732682, 1-6
26. Yong K. S., and Sangmo K., A Review on Mixing in Microfluidics, *Micromachines* 2010, 1, 82-111
27. Mezcua M., Amadeo R. F., Antonio R., Karina B., Pedro L., and Eloy G. C., Chromatographic Methods Applied in the Monitoring of Biodesulfurization Processes-State of the Art, *Talanta*, 73 (2007): 103-114.
28. Wang Y., and Hong C.S., "Effect of hydrogen peroxide, periodate and persulfate on photocatalysis of 2-chlorobiphenyl in aqueous TiO₂ suspensions", *Water Res.*, vol. 33, 9, (1999), 2031-2036.
29. Dixit A., Mungray A. K., and Chakraborty M., Photochemical oxidation of phenol and chlorophenol by UV/H₂O₂/TiO₂ process: A Kinetic Study. *International Journal of Chemical Engineering and applications*, 1(3) 2010
30. Akpan, U.G., and Hameed B.H., Parameters affecting the photocatalytic degradation of dyes using TiO₂-based photocatalysts: A review, *J. Hazard. Mater.*, 170 (2009) 520–529
31. Shiraishi Y., H. Hara, T. Hirai, and I. Komasaawa, A Deep Desulfurization Process for Light Oil by Photosensitizer Oxidation Using a Triplet Photosensitizer and Hydrogen Peroxide in an Oil/Water Two-Phase Liquid-Liquid Extraction System, *Ind. Eng. Chem. Res.*, 1999, 38, 1589-1595.
32. Gemma E. G., Enzymatic degradation of polycyclic aromatic hydrocarbons (PAHs) by manganese peroxidase in reactors containing organic solvents, PhD Dissertation, Chemical Engineering Department, University of Santiago, Spain, 2007.